Effects of molecular and particle scatterings on the model parameter for remote-sensing reflectance

ZhongPing Lee, Kendall L. Carder, and KePing Du

For optically deep waters, remote-sensing reflectance (r_{rs}) is traditionally expressed as the ratio of the backscattering coefficient (b_b) to the sum of absorption and backscattering coefficients ($a + b_b$) that multiples a model parameter (g, or the so-called f'/Q). Parameter g is further expressed as a function of $b_b/(a + b_b)$ (or b_b/a) to account for its variation that is due to multiple scattering. With such an approach, the same g value will be derived for different a and b_b values that provide the same ratio. Because g is partially a measure of the angular distribution of upwelling light, and the angular distribution from molecular scattering is quite different from that of particle scattering; g values are expected to vary with different scattering distributions even if the b_b/a ratios are the same. In this study, after numerically demonstrating the effects of molecular and particle scatterings on the values of g, an innovative r_{rs} model is developed. This new model expresses r_{rs} in two separate terms: one governed by the phase function of molecular scattering and one governed by the phase function of particle scattering, with a model parameter introduced for each term. In this way the phase function effects from molecular and particle scatterings are explicitly separated and accounted for. This new model provides an analytical tool to understand and quantify the phase-function effects on r_{rs}, and a platform to calculate r_{rs} spectrum quickly and accurately that is required for remote-sensing applications. © 2004 Optical Society of America

OCIS codes: 280.0280, 290.1350, 290.5850, 290.5840.

1. Introduction

Ocean color can be measured by subsurface remote-sensing reflectance (r_{rs}),[1–3] which is defined as a ratio of upwelling radiance [$L_u(0-)$] to downwelling irradiance [$E_d(0-)$] at zero depth:

$$r_{rs} = \frac{L_u(0-)}{E_d(0-)}. \quad (1)$$

Since r_{rs} can be evaluated remotely,[4] the relationship between r_{rs} and in-water constituents provides the bridge to estimate water properties analytically from remotely sensed data.

This r_{rs} versus water property relationship can be inexplicitly evaluated by numerical tools such as the Monte Carlo method[5,6] or the HydroLight model.[7] Numerical simulation itself, however, cannot describe explicitly the dependences of ocean color on water property, and the intensive computation limits its feasibility to process global images in satellite remote sensing. To understand the factors that influence ocean color[1,2,8,9] and to implement ocean color algorithms that are based on analytical or semianalytical models,[10–12] a basic requirement is to have an accurate and theoretically based analytical model to link ocean color with water's inherent optical properties.[13,14] Earlier studies[6,15] found some limitations of existing models for remote-sensing reflectance. In this study, we present an improved semianalytical model to describe this relationship.

Through theoretical analyses and numerical modeling,[1–3,6,16] r_{rs} is found generally proportional to the ratio of $b_b/(a + b_b)$. Here a is the absorption coefficient and b_b is the backscattering coefficient of bulk water.[17,18] In remote-sensing applications that require a forward model to calculate r_{rs},[11,12,19,20] the most widely used relationship is the model reported by Gordon *et al.*[5]:

$$r_{rs} = g\,\frac{b_b}{a + b_b}, \quad (2)$$

Z. Lee (zplee@nrlssc.navy.mil) is with the Naval Research Laboratory, Code 7333, Stennis Space Center, Mississippi 39529 and is a visiting professor of ORSI Ocean University of China. K. L. Carder is with the College of Marine Science, University of South Florida, St. Petersburg, Florida 33701. K. Du is with the Ocean Remote Sensing Institute, Ocean University of China, 5 Yushan Road, Qingdao, China.

Received 15 January 2004; revised manuscript received 10 May 2004; accepted 24 May 2004.

0003-6935/04/254957-08$15.00/0

with g expressed as

$$g = g_0 + g_1 \frac{b_b}{a + b_b}, \quad (3)$$

and $g_0 = 0.0949$ and $g_1 = 0.0794$ for nadir-viewed r_{rs}.

There are two limitations for use of the combination of Eqs. (2) and (3) to model r_{rs}. First, only nadir g_0 and g_1 values were provided by Gordon *et al.*,[5] but many sensors measure water color away from nadir to avoid sunglint,[21] and it is known that the angular distribution of r_{rs} is not isotropic.[22,23] Uncertainties arise when using nadir-viewed r_{rs} models to interpret r_{rs} values measured at other angles. Second, Eq. (3) will give the same g value for different a and b_b values as long as they result in the same $b_b/(a + b_b)$ ratio. Note that r_{rs} is a measure of upwelling radiance in a specific direction,[1,7] but b_b is a measure of photons scattered in all backward directions.[24] Depending on sensor solar geometry, r_{rs} could include both forward-scattered and back-scattered photons. Therefore r_s depends on the angular redistribution of scattered photons. When r_{rs} is simplified to a concise form such as Eq. (2), the angular dependence feature of r_{rs} is transferred to parameter g.[1,6,25] Since the redistribution of scattered photons is significantly different between molecular and particle scatterings, the g value that resulted from molecular scattering is expected to differ from that obtained with particle scattering, although both cases can have the same $b_b/(a + b_b)$ ratios. This fact or feature, however, is lost by a model form such as in Eq. (3).

To remedy the above limitations, Morel and Gentili[6] and Morel *et al.*[15] developed a look-up table (LUT) for different solar zenith angles and sensor viewing angles and for different wavelengths and chlorophyll concentrations. This LUT, however, covers only a few wavelengths and chlorophyll concentrations. Because of the nonlinear nature of r_{rs} with wavelength and chlorophyll concentration,[6,26] it is not clear how to interpolate or extrapolate the LUT for wavelengths or chlorophyll concentrations that are not included in the LUT. More importantly, the chlorophyll-based LUT was developed by use of empirical relationships that express water's optical properties (absorption, scattering) as functions of chlorophyll concentration.[6,26] For example, the absorption coefficient of gelbstoff at 440 nm [$a_g(440)$] is fixed explicitly (20% of the absorption coefficient of chlorophyll at 440 nm[6,26]) or inexplicitly[15] as a function of chlorophyll concentration, as is particle scattering.[6,15] It is then difficult to apply the LUT to waters that do not follow these predefined exclusive case-1 relationships,[27] especially for waters in a coastal area.[28] Actually, in ocean color remote sensing it is not known whether the optical properties of a study area follow the statistically derived relationships before the values are derived. An r_{rs} model, with the different scattering-distribution effects accounted for and applicable to more wavelengths and a wider range of waters with less restriction, is certainly desired for ocean color research and remote-sensing applications.

Here we first illustrate numerically the effects of molecular and particle scatterings on the values of g. To overcome some of the limitations of the traditional model, we developed an innovative semianalytical r_{rs} model. The model mimics closely the contributions of molecular and particle scatterings to r_{rs} and accurately reproduces the reflectance spectra generated by Hydrolight. Also, as the model is based on absorption and backscattering properties instead of chlorophyll concentrations, it can be applied to a wider range of waters not limited to case-1 water, as long as absorption and scattering properties are provided.

Table 1. Values Used in the HydroLight Simulations

Variable	Input
Solar zenith angle	30°
$[C]$ (mg m^{-3})	0.03, 0.1, 0.5, 1.0, 5.0, 10.0, 30.0
F	0.2, 0.8, 2.5
B_p	0.1, 0.3, 1.0
λ (nm)	400–700 every 20 nm

2. HydroLight Simulations

Because of multiple scattering, it is difficult (if not impossible) to derive exact g values from the radiative transfer equation, unless the light field can be determined by single scattering.[1,29] As in earlier studies,[6,13] values of g were derived from numerically simulated r_{rs} for different values of a and b_b, by use of a widely accepted HydroLight numerical model[18,30] to compute a subsurface light field. As an example, results with the Sun positioned at 30° from zenith, a wind speed of 5 m/s and a sensor viewing at nadir were used to demonstrate g variations and subsequent analysis and modeling. Table 1 summarizes the properties and wavelengths used in the HydroLight calculations, where the absorption coefficients for pure water were taken from Pope and Fry,[31] pigment concentration ($[C]$) varies from 0.03 to 30.0 mg/m^3 to obtain a wide range of absorption and scattering coefficients, and the water column is assumed infinitely deep and homogeneous.

In the HydroLight simulations, bottom reflectance and inelastic scatterings (such as Raman scattering) are excluded as they are beyond the scope of this study. Their contributions to r_{rs} are discussed by Sathyendranath *et al.*,[32] and by Lee *et al.*[33,34] The solar input and spectral bio-optical models used in the calculations are those provided in the HydroLight model, with adjustments made with regard to the generation of $a_g(440)$ and $b_p(550)$ (particle scattering coefficient at 550 nm). In the Hydrolight simulations, $a_g(440)$ is modeled as $a_g(440) = F\ a_\phi(440)$ [$a_\phi(440)$ is the absorption coefficient of phytoplankton pigments at 440 nm] with a default F value of 0.2 for all waters. In the calculations reported here, F values of 0.2, 0.8, and 2.5 were used to observe their

effects on the values of g, since F is not a constant for both coastal and oceanic waters.[28,35–37]

As in many earlier studies,[5,7,16,27,38] water scattering is separated as scattering from water molecules and scattering from suspended particles (anything other than molecules), with a phase function for particle scattering from Mobley.[18] Further, $b_p(550)$ is expressed as[16,27]

$$b_p(550) = B_p[C]^{0.62}, \quad (4)$$

where B_p is a model parameter with a default value of 0.3 in HydroLight. In the calculations here, B_p values of 0.1, 0.3, and 1.0 were used to observe their effects on g. This B_p variation is based on the facts presented by Gordon and Morel[16] and by Loisel and Morel,[39] where the B_p values varied from less than 0.1 to more than 1.0 when $b_p(550)$ is simply expressed as a function of $[C]$. This is not a surprise since particle scattering (b_p) includes all the scattering effects other than molecular scattering, which includes scattering by phytoplankton,[16] bacteria,[40] suspended sediments,[16] and bubbles.[41] Therefore a fixed B_p value in Eq. (4) is inadequate to describe the b_p variation of natural waters. Since we used a wide range of B_p values in this study, the input b_p is actually an independent variable not restricted by the case-1 assumptions.[27]

Note that the light field is actually determined by absorption and scattering properties;[7] the bio-optical models and the $[C]$ values used in the HydroLight simulations merely to provide a wide range of optical properties.[38] When r_{rs} is modeled as a function of absorption and scattering properties, how the absorption and scattering coefficients relate exactly to phytoplankton concentration is beyond the scope of this study, as long as the absorption and scattering coefficients cover an adequate dynamic range.

3. Values and Variations of g

From the calculated r_{rs} and the input a and b_b values, we easily derived values of g by using Eq. (2). As examples, Figs. 1(a) and 1(b) present the influence of different F and B_p values on the values of g, where $[C]$ is set as 1.0 mg/m^3. Clearly, for a given $[C]$ value, different F and B_p values change the absorption and scattering properties of the water (as normally observed in the field[28]). Consequently g values could vary by as much as 30% for the same $[C]$. More variations are especially found in the blue-green domain, where spectral bands are used to retrieve water properties from water color.[16] Therefore it is necessary to be cautious when applying r_{rs} models that have only a $[C]$ value as a variable if fewer uncertainties are desired.

It is always interesting to know how existing models perform in the generation of r_{rs} spectra for given spectra of a and b_b. For this purpose, Fig. 2 presents examples of r_{rs} from HydroLight computations and r_{rs} from two models. In Fig. 2(a) we used Eqs. (2) and (3) to model r_{rs} and in Fig. 2(b) we used the model of Jerome *et al.*,[3] where r_{rs} is empirically modeled as

$$r_{rs} = -0.00042 + 0.112\frac{b_b}{a} - 0.0455\left(\frac{b_b}{a}\right)^2. \quad (5)$$

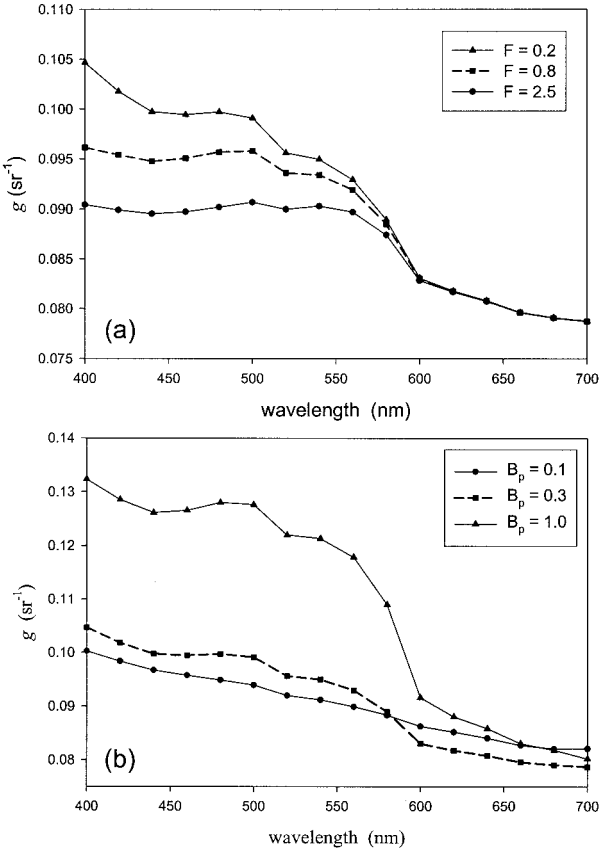

Fig. 1. Variation of g spectra (nadir viewed) for different input parameters. In both (a) and (b) $[C] = 1.0$ mg/m^3, in (a) $B_p = 0.3$ and F varies, in (b) $F = 0.2$ and B_p varies.

In general, both models performed reasonably well for these sample r_{rs} spectra. The r_{rs} spectra obtained with Eqs. (2) and (3) is approximately 10–20% higher than Hydrolight r_{rs} for the longer wavelengths, where particle scattering usually dominates. The r_{rs} spectra obtained with Eq. (5), however, due to its empirical formulation, can result in significantly erroneous r_{rs} values when b_b/a is small. The larger errors in the longer wavelengths could result in extra uncertainties in atmospheric properties if inaccurate r_{rs} values are applied to processes for atmospheric correction.[42]

Figure 3 presents Hydrolight-derived g values of this study, which cover $b_b/(a + b_b)$ up to 0.38 with varying fractions of gelbstoff absorption and various relative contributions of particle scattering. Also shown in Fig. 3 are the g values modeled by Eq. (3). As indicated in earlier studies,[6,43] g values generally range from 0.08 to 0.15 sr^{-1} for an average particle phase function,[18] and generally follow a pattern described by Eq. (3). In contrast to Eq. (3), however, multiple g values were found for the same $b_b/(a + b_b)$

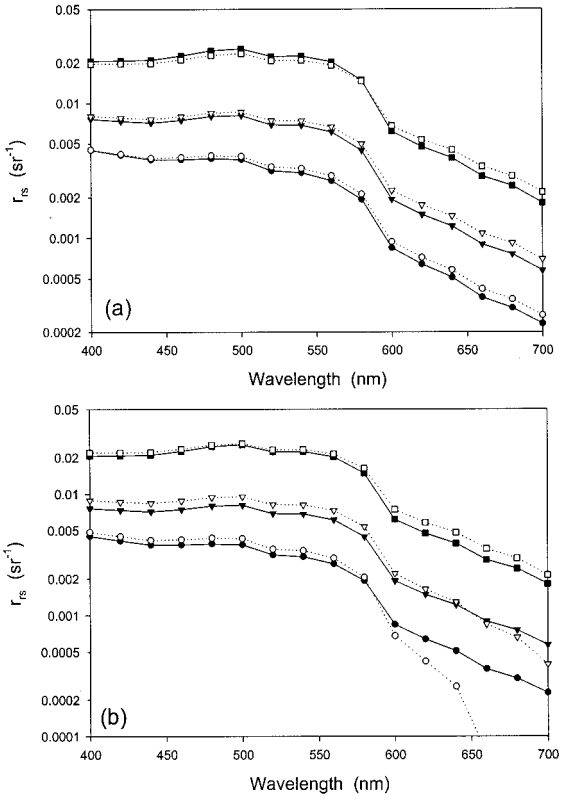

Fig. 2. Nadir-viewed r_{rs} from HydroLight compared with r_{rs} from semianalytical models: (a) r_{rs} is modeled by Eqs. (2) and (3) and (b) r_{rs} is modeled by Eq. (5). In both (a) and (b) $[C] = 1.0$ mg/m^3, $F = 0.8$, B_p varies from 0.1 (circles) and 0.3 (triangles down) to 1.0 (squares).

ratios. The scatter of a g value is more pronounced for cases with $b_b/(a + b_b) < 0.1$, and most oceanic waters fall within this range.[44]

Multiple g values are due mainly to the fact that g depends on the angular distribution of the water volume scattering function (β).[1,7] Recall that water scattering is separated into scatterings by water molecules and scatterings by particles, resulting in a β of the water medium as $\beta = \beta_w + \beta_p$.[6,18] β_w (volume scattering function of water molecules) is a constant background,[18,45] but β_p (volume scattering function of particles) increases with concentrations of particles. Since the angular distribution is significantly different between β_w and β_p,[18] the angular distribution of β varies with the amount of particles present in the water (see Fig.1 in Morel and Loisel[46]). For two cases, as an example, assume that they have the same $b_b/(a + b_b)$ ratios. But, depending on the combination of β_w and β_p, β of one case can be dominated by β_w whereas β of another case can be dominated by β_p, therefore resulting in different g values. Since r_{rs} is described as a simple product of g and $b_b/(a + b_b)$, the existing models for r_{rs} [such as Eqs. (2) and (3) or Eq. (5)] are apparently insufficient to cope with the change in angular distribution of β that resulted from the increase of β_p.

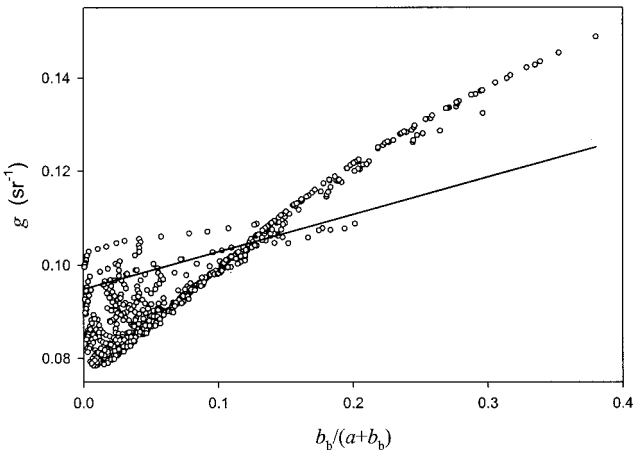

Fig. 3. Traditional g [Eq. (2)] from HydroLight-simulated r_{rs} (viewed at nadir). As expected from theory, multiple g values exist for the same $b_b/(a + b_b)$ ratios. The solid line represents values from Eq. (3).

4. r_{rs} Model with Separate g Parameters

Based on $\beta = \beta_w + \beta_p$ and in an approach analogous to Eq. (2), we can rewrite Eq. (2) as follows to incorporate the β_p-introduced angular variation:

$$r_{rs} = g_w \frac{b_{bw}}{a + b_b} + g_p \frac{b_{bp}}{a + b_b}. \quad (6)$$

Here $b_b = b_{bw} + b_{bp}$ and b_{bw} and b_{bp} are the backscattering coefficients for water molecules and suspended particles, respectively. g_w and g_p are two independent model parameters for molecular scattering and particle scattering, with molecule–particle interscatterings embedded implicitly into both terms.

Comparing Eq. (2) with Eq. (6) yields the expression for the traditional g [Eq. (3)]:

$$g = g_w \frac{b_{bw}}{b_b} + g_p \frac{b_{bp}}{b_b}. \quad (7)$$

The traditional g value is now partitioned and weighted by a molecular contribution (b_{bw}) and a particle contribution (b_{bp}), as Morel and Loisel[46] did when they described the influence of molecular scattering on the model parameters for the downwelling diffuse attenuation coefficient. The g value will approach that determined by molecular scattering (g_w) when particle scattering is negligible (oceanic waters at blue wavelengths, for example), and will approach that determined by particle scattering when molecular scattering is negligible (sediment-abundant coastal waters, for example). Therefore, the g variation that resulted from the change in angular distribution of β is now considered, at least to first order.

The values and variations of the newly introduced model parameters (g_w and g_p), however, are not yet known. To determine their values and variations, the above HydroLight simulated data best serves the purpose.

An initial g_w value was derived by linear regression

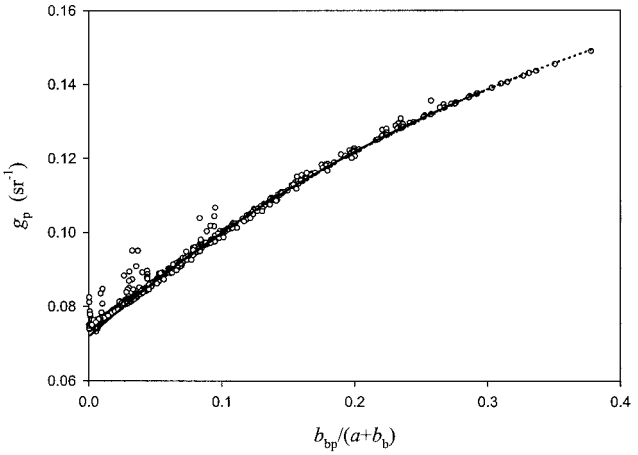

Fig. 4. Calculated g_p values (open circles) with g_w set as the initial value of 0.1107 sr^{-1}. Most of the g_p values are quite predictable with the values of $b_{bp}/(a + b_b)$ (dotted curve), except a few points fall slightly out of the g_p versus $b_{bp}/(a + b_b)$ pattern (see text for discussion).

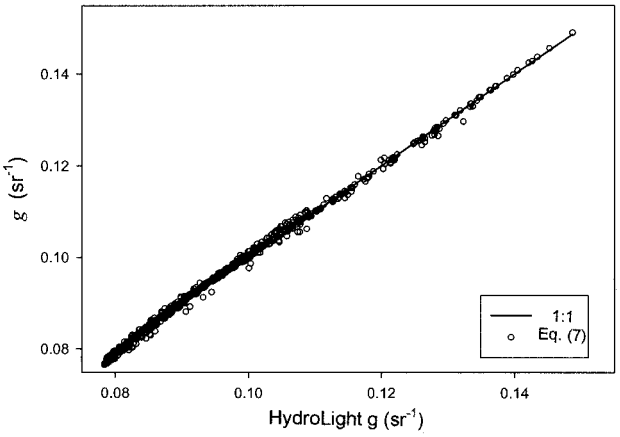

Fig. 5. g values (of nadir-viewed r_{rs}) from HydroLight compared with g values modeled by a combination of Eqs. (7) and (8).

analysis, which used values of b_{bp}/b_b as the independent and values of g as the dependent [Eq. (7)]. The g versus b_{bp}/b_b data came from Hydrolight simulations of $[C] = 0.03$ mg/m^3 with $B_p = 0.1$, and the intercept of 0.1107 sr^{-1} of the linear regression (where $b_{bp} = 0$) became the initial g_w. By applying this initial g_w (0.1107) into Eq. (7), we easily calculated values of g_p. Figure 4 presents these calculated g_p values versus values of $b_{bp}/(a + b_b)$. Clearly, values of g_p are not a constant and generally increase with the ratio of $b_{bp}/(a + b_b)$ to account for the contributions that resulted from multiple scatterings [similar to g versus $b_b/(a + b_b)$ shown in Fig. 3]. Compared with the relationship between g and $b_b/(a + b_b)$ shown in Fig. 3, however, g_p values follow a much tighter and predictable pattern with $b_{bp}/(a + b_b)$ (the dotted curve in Fig. 4), although some residual scatter points still exist. These scatters occur because the 0.1107 initial g_w value has practically no particle scattering. When particle scattering exists, so does molecule–particle interscattering. For such a case, we should expect the actual g_w value to be larger than the initial 0.1107 to include a portion of the interscatterings, unless a third term is introduced specifically for this interscattering contribution, as is done in atmospheric correction algorithms.[47]

To model r_{rs} analytically as a function of absorption and backscattering coefficients, the g_p versus $b_{bp}/(a + b_b)$ relationship (Fig. 4) can be adequately described by use of

$$g_p = G_0\left[1 - G_1\exp\left(-G_2\frac{b_{bp}}{a + b_b}\right)\right], \qquad (8)$$

where G_0, G_1, and G_2 are constants for the specified light geometry and particle phase function. Since our purpose is to provide an r_{rs} model that is consistent with theory and is accurate in the generation of r_{rs} for given absorption and scattering properties, the combination of g_w and (G_0, G_1, G_2) that minimizes the r_{rs} model error achieves this goal. Therefore, values of g_w and (G_0, G_1, G_2) were rederived by best fitting the HydroLight-derived g values with a combination of Eqs. (7) and (8), as was done in the earlier studies to derive values of model parameters.[3,5,13] The resulting values for nadir-viewed r_{rs} are $g_w = 0.113$ and $(G_0, G_1, G_2) = (0.197, 0.636, 2.552)$. As expected, the new g_w value is slightly larger than its initial value, since it also includes some of the contributions from molecule–particle interscatterings.

Figure 5 presents g values modeled from Eqs. (7) and (8) versus those calculated from HydroLight simulations. As expected, g values from the model match the g values from HydroLight excellently, with an average difference of 0.9% (1953 total points). As r_{rs} is also a simple product of g and $b_b/(a + b_b)$ [Eq. (2)], more accurate r_{rs} values can now be obtained semianalytically. Note that, since there are multiple g values for the same $b_b/(a + b_b)$ ratio (Fig. 3), a simple change in the values of g_0 and g_1 in Eq. (3) cannot provide a monotonic relationship between g and $b_b/(a + b_b)$. And, because of the existence of multiple g values for the same $b_b/(a + b_b)$ ratio, dif-

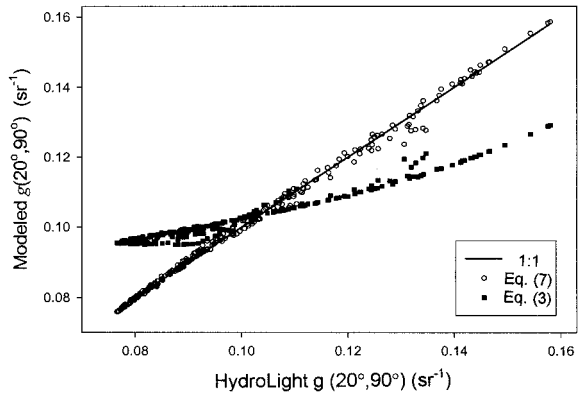

Fig. 6. Same as Fig. 5 but g is for r_{rs} viewed at 20° (subsurface) from nadir and 90° from the solar plane.

Table 2. Model Parameters for Sun at 30° and the Average Particle Phase Function

Viewing Angle	g_w	G_0, G_1, G_2
Nadir	0.113	0.197, 0.636, 2.552
20° (0−) from nadir, 90° from solar plane	0.111	0.189, 0.627, 3.204

ferent g_0 and g_1 values were derived from different g versus $b_b/(a + b_b)$ data sets.[5,43]

So far only model results for nadir-viewed r_{rs} have been presented. As an example, Fig. 6 presents HydroLight calculated and the analytical functions modeled g values for r_{rs} values measured at 20° (subsurface) from nadir and 90° from the solar plane, because many field measurements are collected in such an orientation.[21,48,49] As shown for r_{rs} at nadir, Eq. (3), which was developed for nadir-viewed r_{rs}, cannot accurately model the g values of these simulations. Using Eqs. (7) and (8), HydroLight g is accurately reproduced (average difference is ~ 1%), given a slightly different set of model values: g_w = 0.111 and (G_0, G_1, G_2) = (0.189, 0.627, 3.204). Clearly, Eqs. (7) and (8) can be used to reproduce HydroLight-derived g values for different illumination and viewing geometries by varying the parameter values appropriately. Therefore the analytical r_{rs} function [Eq. (6)] can be used in remote-sensing algorithms for efficient image processing without losing much accuracy in the generation of r_{rs} spectra.

5. Conclusions

From results of numerical simulations it is found that the traditional simple model for parameter g [functions such as Eq. (3)] is insufficient to describe its variation. Basically, because of different angular distributions between molecular and particle scatterings, multiple g values exist for the same $b_b/(a + b_b)$ value. The simple g model such as Eq. (3), however, will always refer to one g value for a $b_b/(a + b_b)$ ratio. Further, when different portions of the g versus $b_b/(a + b_b)$ data set were used for the derivation of g_0 and g_1, different values were obtained.[5,43]

To overcome a shortfall of the traditional approach, an innovative r_{rs} model has been developed. This model still describes r_{rs} as a function of absorption and backscattering coefficients, but, instead of the traditional simple term, this model uses separate parameters to account explicitly for the distribution effects on r_{rs} that result from molecular scattering and particle scattering. The form of the model is, in principle, consistent with the radiative transfer theory. With values of model parameters derived from HydroLight simulations, the model thus provides an explicit tool to better understand and quantify the contributions of molecular and particle scatterings to remote-sensing reflectance, and to cope easily with the multiple g values that exist for the same b_b/a ratio.

The new r_{rs} model [Eq. (6)] has a maximum error of ~3.5% and an average error of ~0.9% for nadir-viewed r_{rs} in this study. Therefore, for given optical properties, the new model provides r_{rs} spectra that closely match theoretical values. This is an important and useful improvement for reaching the desired goal of remotely estimating chlorophyll concentration to within 35%.[50] And, as r_{rs} is expressed as a simple analytical function of absorption and backscattering coefficients, it can be applied to ocean optics studies and remote-sensing algorithms to calculate r_{rs} spectrum efficiently.

Table 2 lists the model parameter values (g_w, G_0, G_1, and G_2) for two viewing geometries and one particle phase function. Parameter tables for various light geometries and particle phase functions can be developed as well, which can then be used in modeling of remote-sensing reflectance and ocean color algorithms over a wide range of waters. As the values of these model parameters (G_0, G_1, and G_2) more or less vary with the shape of the particle phase function, the challenge that follows, especially in ocean color remote sensing, is to know how to assign proper and accurate particle phase functions to different waters. Extensive measurements and classification of biogeochemical provinces[51,52] can provide clues for the assignment. Also, since it is difficult to know precisely the actual particle phase function from remote sensing, the effects of an incorrect phase function assignment to the retrieval of absorption and scattering properties from remote sensing will be analyzed in the future. Nevertheless, the new r_{rs} model developed here provides more insight and understanding with regard to the contributions of molecular and particle scatterings to r_{rs}.

Financial support was provided by the following contracts and grants to Kendall Carder: NASA through NAS5-97137, NAS5-31716, and NAG5-3446; the Office of Naval Research through N00014-96-I-5013 and N00014-97-0006 and support was also provided to Z. Lee by the Naval Research Laboratory through the Hyperspectral Character of the Coastal Zone Program (0601153N). The authors are extremely grateful to Curtis Mobley for providing the HydroLight code and assistance for its use and to the comments of two anonymous reviewers. This study was initiated from a discussion with Howard R. Gordon in Hawaii in October 1998.

References

1. J. R. V. Zaneveld, "A theoretical derivation of the dependence of the remotely sensed reflectance of the ocean on the inherent optical properties," J. Geophys. Res **100,** 13135–13142 (1995).
2. S. Sathyendranath and T. Platt, "Analytic model of ocean color," Appl. Opt. **36,** 2620–2629 (1997).
3. J. H. Jerome, R. P. Bukata, and J. R. Miller, "Remote sensing

reflectance and its relationship to optical properties of natural waters," Int. J. Remote Sensing **17,** 3135–3155 (1996).
4. R. W. Austin, "Inherent spectral radiance signals of the ocean surface," in *Ocean Color Analysis,* **SIO Ref. 74-10** (Scripps Institution of Oceanography, La Jolla, Calif, 1974).
5. H. R. Gordon, O. B. Brown, R. H. Evans, J. W. Brown, R. C. Smith, K. S. Baker, and D. K. Clark, "A semianalytic radiance model of ocean color," J. Geophys. Res. **93,** 10909–10924 (1988).
6. A. Morel and B. Gentili, "Diffuse reflectance of oceanic waters. II. Bidirectional aspects," Appl. Opt. **32,** 6864–6879 (1993).
7. C. D. Mobley, L. K. Sundman, and E. Boss, "Phase function effects on oceanic light fields," Appl. Opt. **41,** 1035–1050 (2002).
8. J. R. V. Zaneveld, "Remotely sensed reflectance and its dependence on vertical structure: a theoretical derivation," Appl. Opt. **21,** 4146–4150 (1982).
9. F. E. Hoge, P. E. Lyon, C. D. Mobley, and L. K. Sundman, "Radiative transfer equation inversion: theory and shape factor models for retrieval of oceanic inherent optical properties," J. Geophys. Res. **108**(C12), 3386, doi:3310.1029/2000JC000447 (2003).
10. K. L. Carder, S. K. Hawes, K. A. Baker, R. C. Smith, R. G. Steward, and B. G. Mitchell, "Reflectance model for quantifying chlorophyll *a* in the presence of productivity degradation products," J. Geophys. Res. **96,** 20599–20611 (1991).
11. S. A. Garver and D. Siegel, "Inherent optical property inversion of ocean color spectra and its biogeochemical interpretation 1. Time series from the Sargasso Sea," J. Geophys. Res. **102** (C8), 18607–18626 (1997).
12. C. S. Roesler and M. J. Perry, "*In situ* phytoplankton absorption, fluorescence emission, and particulate backscattering spectra determined from reflectance," J. Geophys. Res. **100** (C7) 13279–13294 (1995).
13. H. R. Gordon, O. B. Brown, and M. M. Jacobs, "Computed relationships between the inherent and apparent optical properties of a flat homogeneous ocean," Appl. Opt. **14,** 417–427 (1975).
14. R. W. Preisendorfer, *Hydrologic Optics, Vol. 1: Introduction* (National Technical Information Service, Springfield, Va., 1976).
15. A. Morel, D. Antoine, and B. Gentili, "Bidirectional reflectance of oceanic waters: accounting for Raman emission and varying particle scattering phase function," Appl. Opt. **41,** 6289–6306 (2002).
16. H. R. Gordon and A. Morel, *Remote Assessment of Ocean Color for Interpretation of Satellite Visible Imagery: a Review* (Springer-Verlag, New York, 1983), p. 44.
17. J. T. O. Kirk, *Light and Photosynthesis in Aquatic Ecosystems* (Cambridge University, Cambridge, England, 1994).
18. C. D. Mobley, *Light and Water: Radiative Transfer in Natural Waters* (Academic, New York, 1994), p. 111.
19. F. E. Hoge and P. E. Lyon, "Satellite retrieval of inherent optical properties by linear matrix inversion of oceanic radiance models: an analysis of model and radiance measurement errors," J. Geophys. Res. **101** (C7), 16631–16648 (1996).
20. S. Maritorena, D. A. Siegel, and A. R. Peterson, "Optimization of a semianalytical ocean color model for global-scale applications," Appl. Opt. **41,** 2705–2714 (2002).
21. J. L. Mueller, C. Davis, R. Arnone, R. Frouin, K. L. Carder, Z. P. Lee, R. G. Steward, S. Hooker, C. D. Mobley, and S. McLean, "Above-water radiance and remote sensing reflectance measurement and analysis protocols," in *Ocean Optics Protocols for Satellite Ocean Color Sensor Validation*, Revision 3, NASA/TM-2002-210004, J. L. Mueller and G. S. Fargion, eds. (NASA Goddard Space Flight Center, Greenbelt, Md., 2002), pp. 171–182.
22. K. J. Voss, A. Chapin, M. Monti, and H. Zhang, "Instrument to measure the bidirectional reflectance distribution function of surfaces," Appl. Opt. **39,** 6197–6206 (2000).
23. A. Morel, K. J. Voss, and B. Gentili, "Bidirectional reflectance of oceanic waters: a comparison of modeled and measured upward radiance fields," J. Geophys. Res. **100,** 13143–13150 (1995).
24. H. R. Gordon, R. C. Smith, and J. R. V. Zaneveld, "Introduction to ocean optics," in *Ocean Optics VI*, S. Q. Duntley, ed., Proc. SPIE **208,** 14–55 (1979).
25. A. Morel and S. Maritorena, "Bio-optical properties of oceanic waters: a reappraisal," J. Geophys. Res. **106,** 7163–7180 (2001).
26. A. Morel and B. Gentili, "Diffuse reflectance of oceanic waters its dependence on Sun angle as influenced by the molecular scattering contribution," Appl. Opt. **30,** 4427–4438 (1991).
27. A. Morel, "Optical modeling of the upper ocean in relation to its biogenous matter content (Case I waters)," J. Geophys. Res. **93,** 10749–10768 (1988).
28. S. Sathyendranath, ed., "Remote Sensing of Ocean Colour in Coastal, and Other Optically-Complex, Waters," *International Ocean-Colour Coordinating Group* (*IOCCG*) *Report No. 3,* (IOCCG, Dartmouth, Canada, 2000).
29. N. K. Hojerslev, "Analytic remote-sensing optical algorithms requiring simple and practical field parameter inputs," Appl. Opt. **40,** 4870–4874 (2001).
30. C. D. Mobley, *Hydrolight 3.0 User's Guide* (SRI International, Menlo Park, Calif., 1995).
31. R. M. Pope and E. S. Fry, "Absorption spectrum (380–700 nm) of pure water. II. Integrating cavity measurements," Appl. Opt. **36,** 8710–8723 (1997).
32. S. Sathyendranath and T. Platt, "Ocean-color model incorporating transspectral processes," Appl. Opt. **37,** 2216–2227 (1998).
33. Z. P. Lee, K. L. Carder, S. K. Hawes, R. G. Steward, T. G. Peacock, and C. O. Davis, "Model for interpretation of hyperspectral remote-sensing reflectance," Appl. Opt. **33,** 5721–5732 (1994).
34. Z. P. Lee, K. L. Carder, C. D. Mobley, R. G. Steward, and J. S. Patch, "Hyperspectral remote sensing for shallow waters. 1: A semianalytical model," Appl. Opt. **37,** 6329–6338 (1998).
35. A. Bricaud, A. Morel, and L. Prieur, "Absorption by dissolved organic matter of the sea (yellow substance) in the UV and visible domains," Limnol. Occanogr. **26,** 43–53 (1981).
36. K. L. Carder, R. G. Steward, G. R. Harvey, and P. B. Ortner, "Marine humic and fulvic acids: their effects on remote sensing of ocean chlorophyll," Limnol. Oceanogr. **34,** 68–81 (1989).
37. D. A. Siegel and A. F. Michaels, "Quantification of non-algal light attenuation in the Sargasso Sea: implications for biogeochemistry and remote sensing," Deep-Sea Res. Part II **43,** 321–345 (1996).
38. J. T. O. Kirk, "Volume scattering function, average cosines, and the underwater light field," Limnol. Oceanogr. **36,** 455–467 (1991).
39. H. Loisel and A. Morel, "Light scattering and chlorophyll concentration in case 1 waters. a reexamination," Limnol. Oceanogr. **43,** 847–858 (1998).
40. D. Stramski and D. A. Kiefer, "Optical properties of marine bacteria," in *Ocean Optics X*, R. W. Spinrad, ed., Proc. SPIE **1302,** 250–268 (1990).
41. X. D. Zhang, M. Lewis, and B. Johnson, "Influence of bubbles on scattering of light in the ocean," Appl. Opt. **37,** 6525–6536 (1998).
42. D. A. Siegel, M. Wang, S. Maritorena, and W. Robinson, "Atmospheric correction of satellite ocean color imagery: the black pixel assumption," Appl. Opt. **39,** 3582–3591 (2000).
43. Z. P. Lee, K. L. Carder, C. D. Mobley, R. G. Steward, and J. S. Patch, "Hyperspectral remote sensing for shallow waters. 2.

Deriving bottom depths and water properties by optimization," Appl. Opt. **38,** 3831–3843 (1999).
44. A. Morel and L. Prieur, "Analysis of variations in ocean color," Limnol. Oceanogr. **22,** 709–722 (1977).
45. A. Morel, "Optical properties of pure water and pure sea water," in *Optical Aspects of Oceanography*, N. G. Jerlov and E. S. Nielsen, eds. (Academic, New York, 1974), pp. 1–24.
46. A. Morel and H. Loisel, "Apparent optical properties of oceanic water: dependence on the molecular scattering contribution," Appl. Opt. **37,** 4765–4776 (1998).
47. H. R. Gordon and M. Wang, "Retrieval of water-leaving radiance and aerosol optical thickness over oceans with SeaWiFS: a preliminary algorithm," Appl. Opt. **33,** 443–452 (1994).
48. K. L. Carder and R. G. Steward, "A remote-sensing reflectance model of a red-tide dinoflagellate off west Florida," Limnol. Oceanogr. **30,** 286–298 (1985).
49. Z. P. Lee, K. L. Carder, T. G. Peacock, C. O. Davis, and J. L. Mueller, "Method to derive ocean absorption coefficients from remote-sensing reflectance," Appl. Opt. **35,** 453–462 (1996).
50. S. B. Hooker and W. E. Esaias, "An overview of the SeaWiFS project," Eos Trans Am. Geophys. Union **74,** 241–246 (1993).
51. T. Platt and S. Sathyendranath, "Oceanic primary production: estimation by remote sensing at local and regional scales," Science **241,** 1613–1620 (1988).
52. S. Sathyendranath, A. Longhurst, C. M. Caverhill, and T. Platt, "Regionally and seasonally differentiated primary production in the North Atlantic," Deep-Sea Res. Part I **42,** 1773–1802 (1995).